

## Robust and Responsive Silk Ionomer Microcapsules

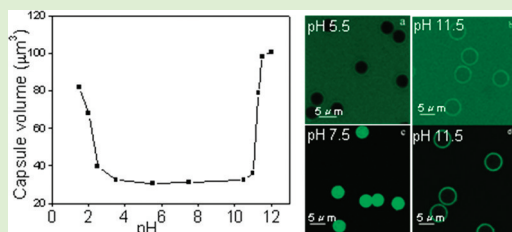
Chunhong Ye,<sup>†,‡</sup> Olga Shchepelina,<sup>‡</sup> Rossella Calabrese,<sup>§</sup> Irina Drachuk,<sup>‡</sup> David L. Kaplan,<sup>§</sup> and Vladimir V. Tsukruk<sup>\*,‡</sup>

<sup>†</sup>School of Chemical Engineering, Nanjing Forestry University, Nanjing, Jiangsu 210037, P. R. China

<sup>‡</sup>School of Materials Science and Engineering, Georgia Institute of Technology, Atlanta, Georgia 30332, United States

<sup>§</sup>Department of Biomedical Engineering, Tufts University, 4, Colby Street, Medford, Massachusetts 02155, United States

**ABSTRACT:** We demonstrate the assembly of extremely robust and pH-responsive thin shell LbL microcapsules from silk fibroin counterparts modified with poly(llysine) and poly(glutamic) acid, which are based on biocompatible silk ionomer materials in contrast with usually exploited synthetic polyelectrolytes. The microcapsules are extremely stable in an unusually wide pH range from 1.5 to 12.0 and show a remarkable degree of reversible swelling/deswelling response in dimensions, as exposed to extreme acidic and basic conditions. These changes are accompanied by reversible variations in shell permeability that can be utilized for pH-controlled loading and unloading of large macromolecules. Finally, we confirmed that these shells can be utilized to encapsulate yeast cells with a viability rate much higher than that for traditional synthetic polyelectrolytes.



### INTRODUCTION

Thin shell microcapsules with responsive properties and controlled permeability have potential applications in the field of drug delivery, biosensing, food industry, biology, and biomedicine.<sup>1–6</sup> The most useful microcapsules for biorelated applications should be biocompatible, noncytotoxic, mechanically robust, and elastic microcapsules, which are stable in a wide range of environmental conditions, have high encapsulation efficiency and controlled or switchable permeability and can be easily prepared.<sup>7</sup> Several approaches have been suggested to fabricate various soft microcapsules, such as interfacial emulsion polymerization,<sup>8</sup> layer-by-layer (LbL) assembly of polymers by H-bonding or covalent bonds,<sup>9</sup> and self-assembly of block copolymers.<sup>2</sup> However, there are a number of common problems associated with these fabrication approaches including high polydispersity, uneven shell coverage, aggregation, and system solidification. Lipid-based liposomes are another approach, but limited stability and low permeability for polar molecules present limitations for general use.<sup>10</sup>

A simple and high yield route using LbL adsorption of oppositely charged polyelectrolytes in decomposable particles, followed by core removal,<sup>11</sup> has been widely used for microcapsule fabrication.<sup>12–14</sup> To date, a series of synthetic polymers, biological components, and nanoparticles has been employed to obtain microcapsules.<sup>15–22</sup> For drug delivery systems, the potential use of microcapsules requires the capability of releasing active compounds at certain pH because some regions of the body have pH lower than normal because of pathological conditions such as inflammation, infection, or malignancy.<sup>23</sup> Furthermore, the microcapsule should be stable for protecting entrapped molecules from degradation or denaturation, biocompatible and biodegradable, which is critical for biosensing applications.<sup>24</sup> The major limitations of

this approach are cytotoxicity of cationic components and poor stability of microcapsules under extreme acidic and basic conditions with capsules heavily irreversibly deformed or dissolved completely.<sup>25,26</sup> Thereby, the choice of proper components for biocompatible microcapsules is limited, and stable and reversibly deformable microcapsules under extreme acidic and basic conditions are rare.

Natural protein, such as silk fibroin (SF), might be considered for construction of such microcapsules. Silk as a natural protein from silkworms and spiders has been widely employed for a variety of biomedical and biotechnological applications.<sup>27,28</sup> The attraction of SF is due to its biocompatible, biodegradable, versatile materials fabrication options and extraordinary mechanical properties.<sup>29–31</sup> Under certain conditions of pH, temperature, or ionic strength, silk proteins form supermolecular structures in the form of hydrogels, films, sponges, fibers, and ropes, which depend on the processing method.<sup>32</sup> Silk-based materials also stabilize the activity of enzymes and biomolecules in harsh environments.<sup>33</sup> Silk capsules have been reported to be formed by an interfacial adsorption method,<sup>34</sup> which was fast and produced robust microcapsules but required the transfer of the capsules from the emulsion into a single-phase solution. Overall, building microcapsules from proteins is challenging because protein assemblies are not very stable in this format. Indeed, our recent study showed the successful fabrication of silk microcapsules via LbL assembly based on hydrophobic–hydrophobic interactions, although they remained modestly robust and stable only within a narrow pH interval.<sup>35</sup>

**Received:** September 6, 2011

**Revised:** October 31, 2011

**Published:** November 3, 2011

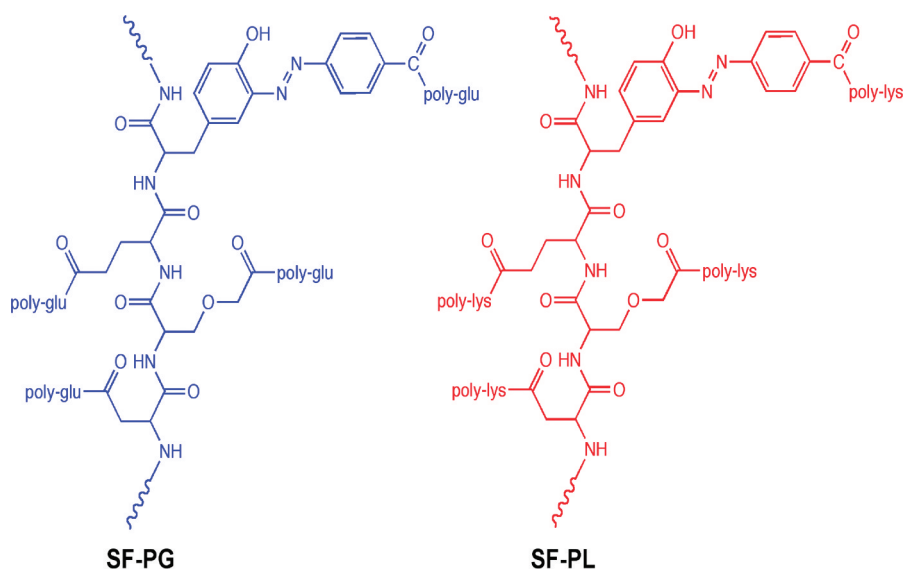


**Figure 1.** Chemical structure of silk-poly(amino acid) ionomers: silk-poly(glutamic) acid (SF-PG) and silk-poly(lysine) (SF-PL) exploited in this study.

Herein we demonstrate robust silk microcapsules that are stable at extreme pH conditions and undergo reversible swelling/deswelling behavior and tunable permeability, all facilitated by additional ionic interactions and cross-linking of silk-based copolymers. These silk ionomer capsules demonstrated pH-triggered responses under extreme acidic (pH < 2.5) and basic (pH > 11.0) conditions with many fold volume increases without compromising capsule disintegration. Such pH-induced changes in capsule size and shell permeability were utilized to demonstrate the encapsulation and release of large macromolecules by changing environmental conditions. Moreover, these shells can be utilized to directly encapsulate yeast cells with a viability rate higher than that for traditional synthetic polyelectrolytes.

## EXPERIMENTAL SECTION

**Materials.** Poly(amino acid)-modified silk materials were obtained using our previously published methods that involve diazonium activation of the abundant tyrosine side chains in the SF chains, followed by chemical linking with polylysine or polyglutamic acid (Figure 1).<sup>32</sup> The SF was extracted from *Bombyx mori* cocoons according to established procedure.<sup>36</sup> First SF was enriched in carboxyl content; then, one of the silk-poly(amino acid)-based ionomers (silk fibroin-polyglutamic acid, SF-PG) was obtained by grafting polyglutamic acid on SF to achieve a high content of carboxyl group. SF-PL represents the SF modified with polylysine to enrich the amine group content.

Silica spheres with a diameter of  $4.0 \pm 0.2 \mu\text{m}$  were obtained from Polysciences as 10% water dispersions. Sodium phosphate dibasic, sodium phosphate monobasic, and hydrofluoric acid (48–51%) were obtained from BDH company. Polyethylenimine (PEI) with  $M_n = 10\,000$  was obtained from Sigma-Aldrich. The cross-linker, 1-ethyl-3-[3-dimethylaminopropyl] carbodiimide hydrochloride (EDC), was obtained from TCI. Fluorescent isothiocyanate (FITC) and FITC-dextran with different molecular weights were purchased from Sigma-Aldrich. The *S. cerevisiae* YPH501 diploid yeast cells were used for cell encapsulation in accordance with usual procedure published elsewhere.<sup>37</sup> In brief, cells were cultured in synthetic minimal medium (SMM) supplemented with necessary nutrients and sugar source, 2% glucose. Cells were harvested at early log phase with optical density (OD)  $\sim 0.3$  to 0.4. Glucose was purchased from Sigma-Aldrich. Live-dead cell staining kit was purchased from Biovision. All solutions were filter-sterilized with polystyrene nonpyrogenic membrane systems

(0.22  $\mu\text{m}$  pore size) (Corning filter system) before applying to the cells. All water used in this study was Nanopure water with resistivity above 18.2  $\text{M}\Omega \text{ cm}$ .

**Fabrication of “PEI(SF-PG/SF-PL)” Capsules.** Silica spheres were dispersed in 0.5 mg/mL PEI solution (prepared in 0.1 M NaCl, pH 7) to make a prime layer to stabilize the LbL process. Then, silica spheres were dispersed in 1 mg/mL SF-PG prepared in 0.05 M phosphate buffer at pH 5.5, followed by three times cycle wash by redispersion in phosphate buffer at pH 5.5 and centrifugation at 1000 rpm for 1 min to remove the excess polyelectrolyte. The SF-PL deposition was carried out by redispersion in 1 mg/mL SF-PL solution, prepared in 0.05 M phosphate buffer at pH 5.5, followed by the same washing procedure described above.

Multilayer capsules were obtained by repeating the alternating deposition of SF-PG and SF-PL components (Figure 2). Each deposition was carried out at a slow rotation avoiding the formation of air bubbles for 15 min, followed by three wash cycles. All capsules presented in this study were cross-linked by introducing 1-ethyl-3-[3-dimethylaminopropyl] carbodiimide hydrochloride (EDC) according to the established procedure.<sup>26</sup> Silica spheres with alternating SF-PG/SF-PL multilayers were added to 5 mg/mL EDC solution (prepared in 0.05 M phosphate buffer at pH 5.5) for 40 min, then washed with phosphate buffer at pH 5.5 to remove the excess coupling agent. To dissolve silica cores, the particles were exposed to HF/ $\text{NH}_4\text{F}$  solution (pH  $\approx 5.5$ ) overnight, followed by dialysis against Nanopure water at pH 5.5 for 72 h (Figure 2).<sup>32,38,39</sup>

**Zeta Potential Measurements.** Surface potentials of silica sphere after every deposited layer and hollow capsules at a wide pH range from 1.5 to 12 were measured on a Zetasizer Nano-ZS (Malvern). Each value was obtained by averaging three independent measurements of 30 runs each.

**Atomic Force Microscopy (AFM).** Surface topography of the hollow capsules in dry state was examined on AFM.<sup>40</sup> The height and phase images were collected from a Dimension-3000 (Digital Instruments) in tapping mode using silicon V-shape cantilevers having a spring constant of 46 N/m. The capsule single-wall thickness was determined as half of the height of the collapsed flat regions on dried capsules using bearing analysis from NanoScope software to generate height histograms.<sup>41,42</sup>

**Scanning Electron Microscopy (SEM).** SEM analysis was performed on a Hitachi S-3400-II scanning electron microscope at 10 kV. Before imaging, capsules were air-dried on a pre-cleaned silicon wafer and sputter-coated with a gold layer.

**Confocal Laser Scanning Microscopy (CLSM).** Confocal images of capsules were obtained with a LSM 510 Vis confocal

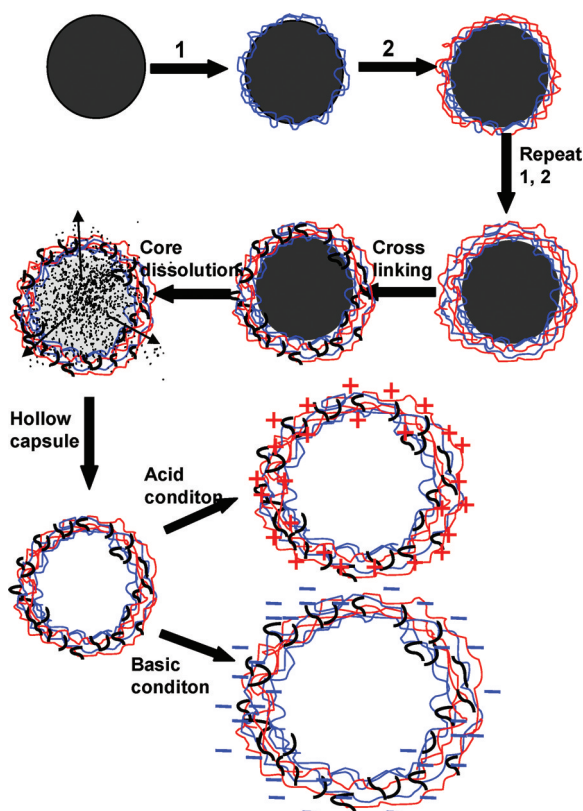


**Figure 2.** Schematic illustration of the procedure for preparation of silk ionomer microcapsules.

microscope equipped with  $63\times 1.4$  oil immersion objective lens (Zeiss). Capsules were visualized by adding FITC solution (1 mg/mL in phosphate buffer at pH 5.5) to the capsule suspension in Lab-Tek chambers (Electron Microscopy Science). Excitation/emission wavelengths were 488/515 nm. To investigate capsule pH responsive property, a drop of capsule suspension was added to several Lab-Tek chambers, mixed with a drop of FITC solution (1 mg/mL in phosphate buffer at pH 5.5). Then, the chamber was  $3/4$  filled with 0.05 M phosphate buffer at different pH. To investigate the pH-reversible responsive property, a drop of capsule suspension mixed with FITC at pH 5.5 was added to a Lab-Tek chamber, and the chamber was  $3/4$  filled with phosphate buffer at pH 11.5. After CLSM images were taken, the liquid in the chamber was removed. The chamber was refilled with another phosphate buffer at pH 7.5. Then, this alternative pH treatment cycle was repeated several times. To check capsule permeability to FITC-dextran, a drop of capsule suspension was added to several Lab-Tek chambers, which were then filled with 1 mg/mL FITC-dextran solution (prepared in phosphate buffer at pH 5.5).

**Encapsulation of Cells with Silk Ionomer Shells.** Yeast cells were grown at  $30\text{ }^{\circ}\text{C}$  in a shaker incubator (New Brunswick Scientific) with 225 rpm to bring them to an early exponential phase [with optical density at 600 nm ( $\text{OD}_{600}$  test) = 0.3 to 0.4].<sup>37</sup> For comparison, we encapsulated yeast cell by the same procedure as PEI-(SF-PG/SF-PL) microcapsules mentioned above. Before deposition of the PEI-(SF-PG/SF-PL) shell, yeast cells were harvested in 1.5 mL microcentrifuge tubes at 2000 rpm for 2 min and washed three times in phosphate buffer (0.01 M in 0.1 M NaCl, pH 6). First, a precursor, PEI (0.5 mg/mL in 0.1 M NaCl, pH 7), was employed, followed by consecutive deposition of SF-PG and SF-PL. After deposition of each layer, cells were washed three times by phosphate buffer. Three bilayers were employed in this study, followed by cross-linking with EDC for 20 min. The viability of yeast cells was assessed by using a live-dead cell staining kit. Images were collected with a LSM 510 Vis confocal microscope equipped with  $63\times 1.4$  oil immersion objective lens. The

viability was estimated by counting the number of viable and dead cells in images acquired in different sections.

## RESULTS AND DISCUSSION

Silk-based copolymers utilized here contain oppositely charged lysine (SF-PL) and glutamate acid (SF-PG) alternating layers to facilitate ionic pairing to enhance LbL construction of stable ultrathin shells (Figure 1). These polyelectrolytes have been obtained by selective modification of functional side groups of the silk protein polymer backbone to add either cationic or anionic amino acid pendant groups, as described elsewhere.<sup>32</sup> As has been demonstrated, these silk ionomers are sensitive to controlled complexation in solution and undergoing complexation behavior when exposed to the changing pH conditions, thus providing a means for responsive behavior.<sup>26,32,43,44</sup>

In this study, LbL assembly was carried out at mild pH (pH 5.5, 0.05 M phosphate buffer solution) to minimize structural changes of the capsule and maximize ionic interactions for enhanced stability. Furthermore, all capsules were employed with a PEI prelayer to ensure effective LbL assembly. In addition, covalent cross-linking was introduced between pendant groups of SF-PL and SF-PG using 1-ethyl-3-[3-dimethylaminopropyl] carbodiimide hydrochloride as a cross-linking agent to provide a stable capsule shape while silk ionomers lost negative/positive charge at extreme acidity (pH 1.0 to 2.0) and basicity (pH 11.0 to 12.0) (Figure 2).<sup>26</sup>

To gain a better understanding of the stepwise growth of the multilayer shells on silica spheres at pH 5.5, we monitored  $\zeta$  potential for the particles after each deposition step (Figure 3a).

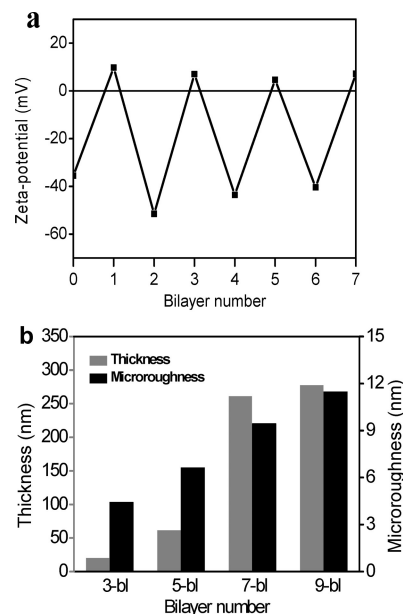


**Figure 3.** (a) Variation in the  $\zeta$ -potential during the fabrication of PEI-(SF-PG/SF-PL)<sub>n</sub> shells on silica spheres; 0 corresponds to the bare silica spheres and 1 corresponds to PEI prelayer. (b) Shell thickness and microroughness for silk ionomer shells with different bilayer numbers.

At pH 5.5, SF-PG is negatively charged ( $\text{pK}_a$  of poly glutamic acid is  $\sim 3.5$ ), whereas SF-PL is positively charged ( $\text{pK}_a$  of polylysine is  $\sim 9$ ).<sup>45</sup> The original silica spheres have a  $\zeta$  potential of around  $-35$  mV. The  $\zeta$  potential alternates after each SF-PG and SF-PL layer deposition, which indicates a

common charge-overcompensated mechanism of LbL shell formation and stepwise growth of silk shells around the silica particles.

The thickness of silk ionomer capsule shells with different number of bilayers was measured by AFM cross sections in dry state (Figures 3b and 4). The AFM images of capsules composed

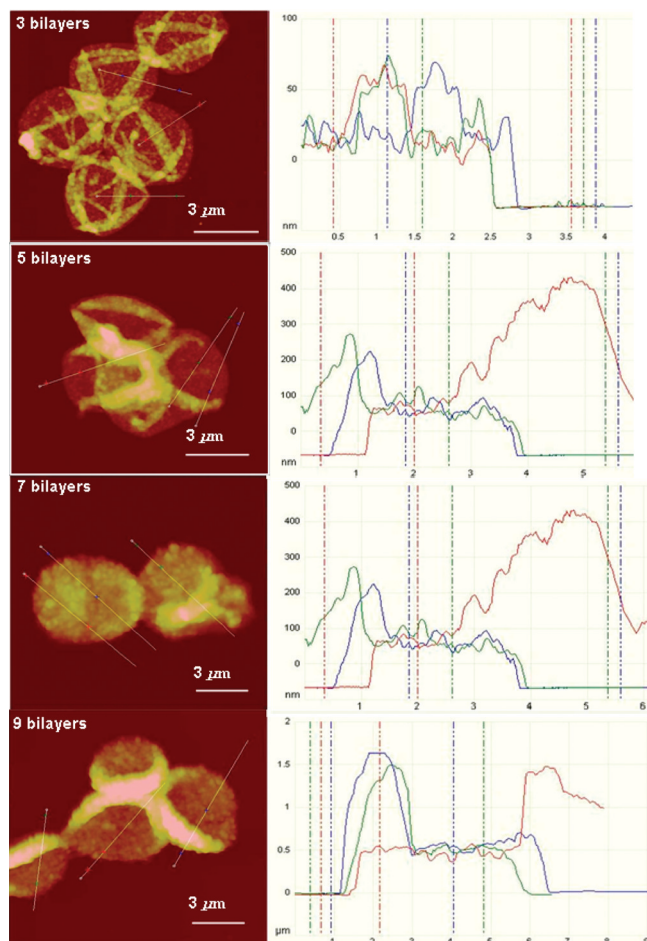


**Figure 4.** AFM cross-section analysis of silk ionomer capsules with different number of bilayers.

of three, five, seven, and nine bilayers, after being placed on a silicon wafer, have been collapsed upon drying with a high degree of random wrinkling due to capillary forces. This observation was confirmed by SEM images of coated particles and silk shells after core release (Figure 5a,b).<sup>46–48</sup>

The shell thickness increased from  $19 \pm 1$  to  $277 \pm 11$  nm with an increasing number of bilayers (Figure 3b). Unlike the silk-on-silk shells based on hydrophobic interactions with a linear growth mode with an average increment of 4 nm per bilayer, the LbL assembly of silk ionomers exhibited an exponential growth, which is common for many biopolyelectrolytes including polylysine/polyglutamic acid LbL films with intense interfacial diffusion processes and efficient complexation.<sup>49–51</sup> The microroughness of shells also increased from 4.4 to 11.4 nm (as measured in selected areas of  $1 \times 1 \mu\text{m}^2$ ), a common phenomenon for diffusion-enhanced LbL assembly with aggregated and porous morphologies.<sup>52</sup>

The drying hollow capsules collapsed because of capillary forces with random folding patterns common for uniform shells (Figure 5).<sup>53,54</sup> High-resolution AFM images revealed a grainy

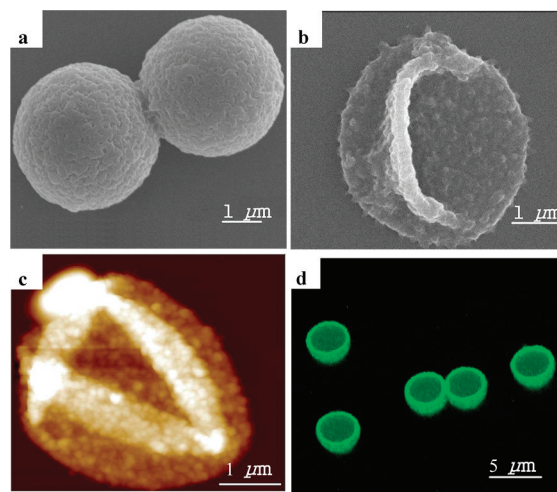


**Figure 5.** Morphology of silk ionomer capsules. (a) SEM image of PEI-(SF-PG/SF-PL)<sub>7</sub> capsule with silica core. (b) SEM image of PEI-(SF-PG/SF-PL)<sub>9</sub> capsule after core dissolution. (c) AFM topography image of dried PEI-(SF-PG/SF-PL)<sub>5</sub> capsule (z-scale: 500 nm). (d) 3D confocal image of the PEI-(SF-PG/SF-PL)<sub>5</sub> capsule shell labeled with FITC.

texture that is associated with the microphase morphology of silk materials undergoing partial transformation of secondary structure during drying.<sup>55</sup> Confocal images of capsule shells labeled by FITC shows the hollow structure of capsule after the silica core is dissolved (Figure 5d). All capsules possess very uniform shapes with diameters around  $3.6 \mu\text{m}$ , which is close to the original core diameter considering some shell contraction.<sup>56</sup>

Next, the silk ionomer capsules were subjected to various pH values to test their stability and responsive behavior. First, the variation of  $\zeta$  potential of capsules at a wide pH range from 1.5 to 12.0 was studied (Figure 6a). The  $\zeta$  potential is a negative

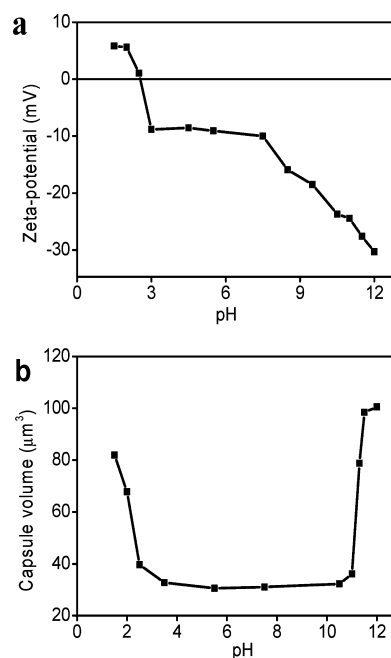


**Figure 6.** pH-induced variations of silk base capsules. (a) The  $\zeta$ -potential for PEI-(SF-PG/SF-PL)<sub>3</sub> hollow capsule as a function of pH. (b) pH-triggered swelling of PEI-(SF-PG/SF-PL)<sub>9</sub> hollow capsule at wide pH range from 1.5 to 12.0.

constant over the pH range from 3.0 to 7.5 and increases to positive values for pH below 2.5 due to the protonation of the carboxyl-terminal group on SF-PG below its  $pK_a$ .<sup>45</sup> Capsule potential becomes excessively negative because of the deprotonation of the amino groups on the SF-PL above pH 9. Correspondingly, the volume of capsules dramatically increases under these terminal conditions (Figure 6b). Capsule diameter with nine bilayers increases from  $3.8 \pm 0.2$  to  $5.3 \pm 0.2$  (pH 1.5) and  $5.7 \pm 0.2 \mu\text{m}$  (pH 12.0) within 10 s after changing pH.

The capsule remains stable with unchanged dimensions in a wide range of pH from 2.5 to 11.0 in striking contrast with synthetic LbL shells with significant changes in the vicinity of neutral pH.<sup>57,58</sup> However, in contrast with conventional capsules that are readily dissolved at extreme pH values, cross-linked silk ionomer capsules with the number of bilayers above 7 are capable of multiple and fully reversible shape changes without any residual deformation (Figure 7). It is

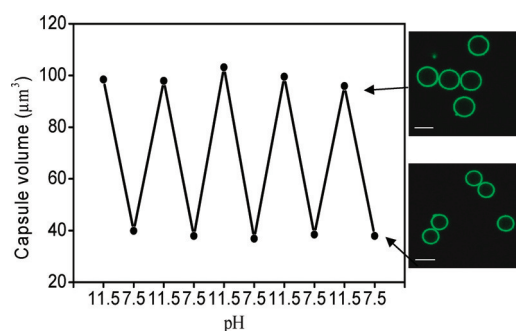


**Figure 7.** Reversible volume responsive property of PEI-(SF-PG/SF-PL)<sub>9</sub> hollow capsules during alternating pH treatment; Arrow indicates the CLSM image of capsules at corresponding pH after five pH cycle treatments. Scale bar is 5  $\mu\text{m}$ .

worth noting that only capsules with additional covalent cross-linked shells demonstrated extreme stability under basic conditions and kept an uniform shape during the reversible pH response, although the capsules without cross-linking totally dissolved when exposed to basicity (pH > 11.5) for 15–20 min.

The porous morphology of the silk ionomer shells facilitates their high permeability, which, in turn, can be controlled by external pH.<sup>59</sup> To test this ability, we exploited the permeability of green-fluorescent FITC-dextran of various molecular weights at pH 5.5 (Table 1).<sup>34,60–62</sup> The thinnest shells

**Table 1. Permeability of PEI-(SF-PG/SF-PL)<sub>n</sub> Capsules with Different Bilayer Numbers to FITC-Dextran Solution with Varied Molecular Weight in Phosphate Solution at pH 5.5<sup>a</sup>**

layer	$M_w$								
	4 kDa	10 kDa	20 kDa	40 kDa	70 kDa	150 kDa	250 Da	500 kDa	2000 kDa
3-bl	+	+	+	+	+	+	+	+	+
5-bl	+	+	+	+	±	–	–	–	–
7-bl	+	–	–	–	–	–	–	–	–
9-bl	+	–	–	–	–	–	–	–	–

<sup>a</sup>Symbols “+”, “–”, and “±” indicate permeable, impermeable, and partially permeable capsules, respectively.

(three bilayers) were permeable to all of the dextrans including 2000 kDa molecular weight, indicating an extremely porous morphology. Increasing the shell thickness resulted in a gradual

decrease in cutoff molecular weight to 4 kDa for a nine bilayer shell, a common trend for LbL capsules, which indicates gradual densification of shells and porosity reduction with increasing shell thickness.

The reported hydrodynamic diameters of FITC-dextran with different molecular weights of 4, 70, 150, and 2000 kDa are 3.30, 11.60, 17.70, and 31.8 nm, respectively.<sup>63</sup> Therefore, we can estimate that the smallest mesh size of the polymer network for the thickest shells is  $\sim 7$  nm, and the largest mesh size of the capsules with three bilayers exceeds 32 nm. The mesh size is easily controlled by the number of silk ionomer bilayers assembled.

Moreover, the loading/unloading behavior of these capsules can be controlled by external pH, as was demonstrated by using FITC-dextran as a fluorescence probe (Figure 8). For instance,

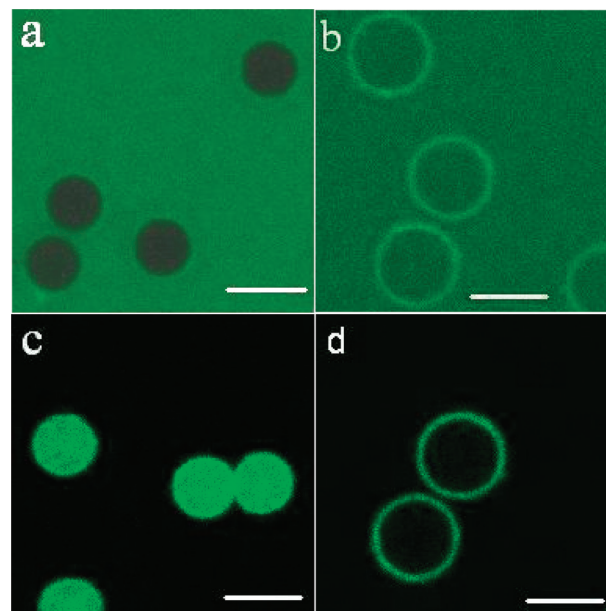


**Figure 8.** Confocal microscopy images of encapsulation and release properties of PEI-(SF-PG/SF-PL)<sub>9</sub> to 20 kDa FITC-Dextran in phosphate solution with different pH conditions. (a) PEI-(SF-PG/SF-PL)<sub>9</sub> capsules exposed to 20 kDa FITC-Dextran solution at pH 5.5. (b) PEI-(SF-PG/SF-PL)<sub>9</sub> capsules exposed to 20 kDa FITC-Dextran solution at pH 11.5. (c) Capsules in panel b adjusted to pH 7.5. (d) Capsules in panel c adjusted to pH 11.5. Scale bar is 5  $\mu\text{m}$ .

20 kDa dextran did not permeate the shells of nine-bilayer capsules at pH 5.5 (Figure 8a), but when the capsules were exposed to the dextran with the same molecular weight at pH 11.5, the “closed” morphology immediately became “open” and highly permeable (Figure 8b). Using this approach, FITC-dextran can be encapsulated by changing the pH of the solution from 11.5 to 7.5 (Figure 8c). The encapsulation is very stable, lasting for at least 2 days. Because this capsule solution was adjusted from pH 7.5 to 11.5 again, the encapsulated dextran can be completely released from capsules in 2 h (Figure 8d).

Finally, we conducted preliminary testing of cytotoxicity of silk ionomer shells by encapsulating yeast cells. As known, high cytotoxicity of synthetic LbL shells is caused by the direct contact of cationic polyelectrolytes with cells, which impose formation of pores in the cell membrane, followed by severe cell damage and death, and thus removal or screening the cationic component has been implemented.<sup>64–66</sup> In the case of

natural polyelectrolytes, such as silk ionomers studied here, yeast cells encapsulated with PEI-(SF-PG/SF-PL)<sub>3</sub> shells maintain viability up to 29% in the case of having a PEI prelayer and being cross-linked with EDC for 20 min. For cells encapsulated without a PEI prelayer and cross-linking agent, viability reached 38%, which is more than two times higher than the 17% viability of cells encapsulated with conventional poly(styrene sulfonate)/poly(allylamine hydrochloride) (PAH/PSS)<sub>3</sub> shells as observed in our previous study.<sup>66</sup> Moreover, a previous cytocompatibility study of SF-PG and SP-PL by in situ gelation encapsulation human cervical fibroblasts demonstrated exceptionally high cell viability reaching 90%.<sup>32</sup> A cell encapsulation study using LbL assembly of natural polyelectrolytes with improved viability will be discussed elsewhere.

## CONCLUSIONS

In conclusion, extremely robust and stable silk ionomer microcapsules were successfully fabricated by combining ionic pairing and covalent cross-linking of functionalized pendant groups. The capsules were stable even under extreme acidic (pH 1.0 to 2.0) and basic (pH 11.0 to 12.0) conditions. The capsules showed significant and highly reversible pH responsive behavior at pH below 2.0 and above 11.0, with the maximum volume swelling reaching 800%. Furthermore, these silk ionomer capsules exhibited pH-triggered permeability, thus facilitating pH-controlled encapsulation and release. In comparison with the previous pH-triggered capsules composed of synthesis polyelectrolytes by H-bonding or electrostatic interactions, which possess swelling/deswelling behavior usually at mild pH and are deformed or totally dissolved under strong acidic/basic conditions,<sup>20,26</sup> the silk-ionomer capsules with the ability to pH-induce encapsulation are important for manipulated loading–unloading of therapeutic cargo and the design of biosensing systems.<sup>67</sup> Thereby, the silk ionomer capsules present a promising platform for stable and tunable microcontainers for encapsulation and delivery of small and large macromolecules, nanoparticles, cells, and other species.

## AUTHOR INFORMATION

### Corresponding Author

\*E-mail. Vladimir@mse.gatech.edu.

## ACKNOWLEDGMENTS

This work was supported by the Air Force Office of Scientific Research FA9550-08-1-0446, FA9550-09-1-0162, FA9550-10-1-0172, and FA9550-11-1-0233 grants, U.S. Department of Energy, Office of Basic Energy Sciences Award no. DE-FG02-09ER46604, and China Scholarship Council 2010832447, Nanjing Forestry University Graduate Student Innovation Program 2011YB012. We thank Dr. Svetlana Harbaugh (Wright Patterson AirForce Base) for providing yeast cells and Dr. Milana Lisunova, Dhaval D. Kulkarni, Zachary A. Combs, and Iljun Choi (Georgia Institute of Technology) for assistance.

## REFERENCES

- (1) Caruso, F.; Caruso, R. A.; Möhwald, H. *Science* **1998**, *282*, 1111–1114.
- (2) Discher, B. M.; Won, Y. Y.; Ege, D. S.; Lee, J. C. M.; Bates, F. S.; Discher, D. E.; Hammer, D. A. *Science* **1999**, *284*, 1143–1146.
- (3) Dinsmore, A. D.; Hsu, M. F.; Nikolaidis, M. G.; Marques, M.; Bausch, A. R.; Weitz, D. A. *Science* **2002**, *298*, 1006–1009.
- (4) Esser-Kahn, A. P.; Odom, S. A.; Sottos, N. R.; White, S. R.; Moore, J. S. *Macromolecules* **2011**, *44*, 5539–5553.
- (5) Bédard, M. F.; Geest, B. G.; Skirtach, A. G.; Möhwald, H.; Sukhorukov, G. B. *Adv. Colloid Interface Sci.* **2010**, *158*, 2–14.
- (6) Stuart, M. A.; Huck, W. T.; Genezer, J.; Müller, M.; Ober, C.; Stamm, M.; Sukhorukov, G. B.; Szleifer, L.; Tsukruk, V. V.; Urban, M.; Winnik, F.; Zauscher, S.; Luzinov, L.; Minko, S. *Nat. Mater.* **2010**, *9*, 101–113.
- (7) Gordon, V. D.; Xi, C.; Hutchinson, J. W.; Bausch, A. R.; Marquez, M.; Weitz, D. A. *J. Am. Chem. Soc.* **2004**, *126*, 14117–14122.
- (8) Jang, J.; Ha, H. *Langmuir* **2002**, *18*, 5613–5618.
- (9) Huang, H. Y.; Remsen, E. E.; Kowalewski, T.; Wooley, K. L. *J. Am. Chem. Soc.* **1999**, *121*, 3805–3806.
- (10) Lasic, D. D. *Liposomes: From Physics to Application*; Elsevier: Amsterdam, 1993.
- (11) Donath, E.; Sukhorukov, G. B.; Caruso, F.; Davis, S. A.; Möhwald, H. *Angew. Chem., Int. Ed.* **1998**, *37*, 2002–2005.
- (12) Skirtach, A. G.; Karageorgiev, P.; Bédard, M. F.; Sukhorukov, G. B.; Möhwald, H. *J. Am. Chem. Soc.* **2008**, *130*, 11572–11573.
- (13) De Cock, L. J.; Koker, S.; Geest, B. G.; Grooten, J.; Vervaeet, C.; Remon, J. P.; Sukhorukov, G. B.; Antipina, M. N. *Angew. Chem., Int. Ed.* **2010**, *49*, 6954–6973.
- (14) Decher, G.; Schlenoff, J. B.; Lehn, J.-M. *Multilayer Thin Films: Sequential Assembly of Nanocomposite Materials*; Wiley-VCH: Weinheim, Germany, 2003; pp 1–524.
- (15) Wong, M. S.; Cha, J. N.; Choi, K. S.; Deming, T. J.; Stucky, G. D. *Nano Lett.* **2002**, *2*, 583–587.
- (16) Kukula, H.; Schlaad, H.; Antomietti, M.; Forster, S. *J. Am. Chem. Soc.* **2002**, *124*, 1658–1663.
- (17) Lee, D.; Rubber, M. F.; Cohen, V. *Chem. Mater.* **2005**, *17*, 1099–1105.
- (18) Kim, B. S.; Vinogradova, O. I. *J. Phys. Chem. B* **2004**, *108*, 8161–8165.
- (19) Sukhorukov, G. B.; Fery, A.; Möhwald, V. *Prog. Polym. Sci.* **2005**, *30*, 885–897.
- (20) Elsner, N.; Kozlovskaya, V.; Sukhishvili, S. A.; Fery, A. *Soft Matter* **2006**, *2*, 966–972.
- (21) Such, G. K.; Tjijto, E.; Postma, A.; Johnston, A. P. R.; Caruso, F. *Nano Lett.* **2007**, *7*, 1706–1710.
- (22) Ochs, C. J.; Such, G. K.; Yan, Y.; Koeberden, M. P.; Caruso, F. *ACS Nano* **2010**, *4*, 1653–1663.
- (23) Leroux, J.; Roux, E.; Garrec, D. L.; Hong, K.; Drummond, D. C. *J. Controlled Release* **2001**, *72*, 71–84.
- (24) Faraji, V.; Wipf, P. *Bioorg. Med. Chem.* **2009**, *17*, 2950–2962.
- (25) Déjurgat, C.; Sukhorukov, G. B. *Langmuir* **2004**, *20*, 7265–7269.
- (26) Kozlovskaya, V.; Kharlampieva, E.; Mansfield, M. L.; Sukhishvili, V. *Chem. Mater.* **2006**, *18*, 328–336.
- (27) Hofmann, S.; Foo, C. T.; Rossetti, F.; Textor, M.; Vunjak-Novakovic, G.; Kaplan, D. L. *J. Controlled Release* **2006**, *111*, 219–227.
- (28) Omenetto, F. G.; Kaplan, D. L. *Nat. Photonics* **2008**, *2*, 641–643.
- (29) Wang, Y.; Kim, H. J.; Vunjak-Novakovic, G.; Kaplan, D. L. *Biomaterials* **2006**, *36*, 6064–6082.
- (30) Omenetto, F. G.; Kaplan, D. L. *Science* **2010**, *329*, 528–531.
- (31) Jin, H. J.; Kaplan, D. L. *Nature* **2003**, *424*, 1056–1061.
- (32) Serban, M. A.; Kaplan, D. L. *Biomacromolecules* **2010**, *11*, 3406–3412.
- (33) Yu, A.; Wang, Y.; Barlow, E.; Caruso, F. *Adv. Mater.* **2005**, *17*, 1737–1741.
- (34) Hermanson, K. D.; Harasim, M. B.; Scheibel, T.; Bausch, A. R. *Phys. Chem. Chem. Phys.* **2007**, *9*, 6442–6446.
- (35) Shchepelina, O.; Drachuk, I.; Gupta, M. K.; Lin, J.; Tsukruk, V. V. *Adv. Mater.* **2011**, *23*, 4655–4660.
- (36) Murphy, A. R.; St. John, P.; Kaplan, D. L. *Biomaterials* **2008**, *29*, 2829–2839.
- (37) Kozlovskaya, V.; Harbaugh, S.; Drachuk, V.; Shchepelina, V.; Kelley-Loughnane, N.; Stone, M.; Tsukruk, V. V. *Soft Matter* **2011**, *7*, 2364–2372.

- (38) Wang, Y. J.; Caruso, F. *Chem. Commun.* **2004**, *40*, 1528–1529.
- (39) Shimizu, K.; Cha, J.; Stucky, G. D.; Morse, D. E. *Proc. Natl. Acad. Sci. U.S.A.* **1998**, *95*, 6234–6238.
- (40) Tsukruk, V. V.; Reneke, D. H. *Polymer* **1995**, *36*, 1791–1808.
- (41) Elsner, N.; Dubreui, F.; Fery, A. *Phys. Rev. E* **2004**, *69*, 031802/1–031802/6.
- (42) McConney, M. E.; Singamaneni, S.; Tsukruk, V. V. *Polym. Rev.* **2010**, *50*, 235–286.
- (43) Shiratori, S. S.; Rubner, M. F. *Macromolecules* **2003**, *33*, 4213–4219.
- (44) Mendelsohn, J. D.; Barrett, C. J.; Chan, V. V.; Pal, A. J.; Mayes, A. M.; Rubner, M. F. *Langmuir* **2000**, *16*, 501–5023.
- (45) Yu, A.; Gentle, V.; Lu, V. J. *Colloid Interface Sci.* **2009**, *333*, 341–345.
- (46) Wang, Y.; Caruso, F. *Chem. Mater.* **2005**, *17*, 953–961.
- (47) Caruso, F. *Chem.—Eur. J.* **2000**, *6*, 413–419.
- (48) Boulmedais, V.; Frisch, B.; Etienne, O.; Lavalle, V.; Picart, C.; Ogier, V.; Voegel, J. C.; Schaaf, P.; Egles, C. *Biomaterials* **2004**, *25*, 2003–2011.
- (49) Laugel, N.; Betscha, C.; Winterhalter, M.; Voegel, V.; Schaaf, P.; Ball, V. *J. Phys. Chem. B* **2006**, *110*, 19443–19449.
- (50) Porcel, C.; Lavalle, Ph.; Ball, V.; Decher, G.; Senger, B.; Voegel, V.; Schaaf, P. *Langmuir* **2006**, *22*, 4376–4383.
- (51) Lavalle, Ph.; Picart, V.; Mutterer, V.; Gergely, V.; Reiss, H.; Voegel, J. C.; Senger, B.; Schaaf, P. *J. Phys. Chem. B* **2004**, *108*, 635–648.
- (52) Jiang, C.; Wang, X.; Gunawidjaja, R.; Lin, Y. H.; Gupta, M.; Kaplan, D. L.; Naik, R. R.; Tsukruk, V. V. *Adv. Funct. Mater* **2007**, *17*, 2229–2237.
- (53) Vinogradova, O. I. *J. Phys: Condens. Matter* **2004**, *16*, R1105–R1134.
- (54) Heuvingh, J.; Zappa, M.; Ferry, A. *Langmuir* **2005**, *21*, 3165–3171.
- (55) Gupta, M. K.; Singamaneni, S.; McConney, V.; Drummy, L. F.; Naik, R. R.; Tsukruk, V. V. *Adv. Mater.* **2010**, *22*, 115–119.
- (56) Shulha, H.; Wang, C. P.; Wang, D. L.; Tsukruk, V. V. *Polymer* **2006**, *47*, 5821–5830.
- (57) Kozlovskaya, V.; Sukhishvili, S. A. *Macromolecules* **2006**, *39*, 6191–6199.
- (58) Mendelsohn, J. D.; Barrett, C. J.; Chan, V. V.; Pal, A. J.; Mayes, A. M.; Rubner, M. F. *Langmuir* **2000**, *16*, 5017–5023.
- (59) Sukhorukov, G. B.; Fery, A.; Brumen, M.; Möhwald, H. *Phys. Chem. Chem. Phys.* **2004**, *6*, 4078–4098.
- (60) Brissova, M.; Petro, M.; Lacik, I.; Powers, A. C.; Wang, T. *Anal. Biochem.* **1996**, *242*, 104–111.
- (61) Robitaille, R.; Leblond, V.; Bourgeois, Y.; Henley, N.; Loignon, M.; Halle, J. P. *J. Biomed. Mater. Res.* **2000**, *50*, 420–427.
- (62) Nuidin, N.; Canaple, L.; Bartkowiak, V.; Desvergne, B.; Hunkeler, D. *J. Appl. Polym. Sci.* **2000**, *75*, 1165–1175.
- (63) Gong, D.; Yadavalli, V.; Padavalli, M.; Paulose, M. *Biomed. Microdevices* **2003**, *51*, 75–80.
- (64) Wilson, J. T.; Cui, W.; Chaikof, E. L. *Nano Lett.* **2008**, *8*, 1940–1948.
- (65) Wilson, J. T.; Cui, W.; Kozlovskaya, V.; Kharlampieva, E.; Pan, D.; Qu, Z.; Krishnamurthy, V. R.; Mets, J.; Kumar, V.; Wen, J.; Song, Y.; Tsukruk, V. V.; Chaikof, E. L. *J. Am. Chem. Soc.* **2011**, *133*, 7054–7064.
- (66) Carter, J. L.; Drachuk, I.; Harbaugh, S.; Kelley-Loughnane, N.; Stone, M.; Tsukruk, V. V. *Macromol. Biosci.* **2011**, *11*, 1244–1253.
- (67) Zhang, F.; Wu, Q.; Chen, V.; Zhang, V.; Lin, X. F. *J. Colloid Interface Sci.* **2008**, *317*, 477–484.